Hybridization effects on the out-of-plane electron tunneling properties of monolayers: is h-BN more conductive than graphene?

2014 Nanotechnology 25 345703

(http://iopscience.iop.org/0957-4484/25/34/345703)

IOP Publishing Nanotechnology
Nanotechnology **25** (2014) 345703 (7pp) doi:10.1088/0957-4484/25/34/345703

Hybridization effects on the out-of-plane electron tunneling properties of monolayers: is h-BN more conductive than graphene?

Xiaoliang Zhong[1], Rodrigo G Amorim[2], Alexandre R Rocha[3] and Ravindra Pandey[1]

[1] Department of Physics, Michigan Technological University, Houghton, Michigan 49931, USA
[2] Physics Department, Uppsala University, Uppsala, Sweden
[3] Instituto de Física Teórica, Universidade Estadual Paulista (UNESP), Sao Paulo, SP, Brazil

E-mail: reilya@ift.unesp.br and pandey@mtu.edu

Received 21 February 2014, revised 9 May 2014
Accepted for publication 3 July 2014
Published 7 August 2014

Abstract

Electron transport properties through multilayers of hexagonal boron nitride (h-BN) sandwiched between gold electrodes is investigated by density functional theory together with the non-equilibrium Green's function method. The calculated results find that despite graphene being a gapless semimetal and h-BN two-dimensional layer being an insulator, the transmission function perpendicular to the atomic layer plane in both systems is nearly identical. The out-of-plane tunnel current is found to be strongly dependent on the interaction at the interface of the device. As a consequence, single layer h-BN coupled with atomically flat weakly interacting metals such as gold may not work as a good dielectric material, but the absence of sharp resonances would probably lead to more stable out-of-plane electronic transport properties compared to graphene.

S Online supplementary data available from stacks.iop.org/NANO/25/345703/mmedia

Keywords: BN monolayer, electron transport, graphene

(Some figures may appear in colour only in the online journal)

1. Introduction

Two-dimensional (2D) nanomaterials with thicknesses of less than a few hundred nanometers have been the subject of great research interest, due to their novel and peculiar properties which are not obtainable in their three-dimensional counterparts [1]. Graphene and monolayer of the hexagonal boron nitride (h-BN) are such representative prototypes of atomically thin 2D nanomaterials [2, 3]. They share the similar planar honeycomb lattice structures, though they exhibit distinct electronic properties. While graphene is a semimetal which has an ultra-high electron mobility at room temperature [4, 5], the h-BN monolayer is deemed as a good dielectric with a band gap of ≈5.5 eV [6]. This is due to the fact that graphene has two symmetric carbon sublattices, with conduction band and valence band just crossing at the so-called Dirac points [7]. In contrast, the h-BN monolayer consists of the asymmetric boron and nitrogen sublattices whose semi-ionic nature leads to a gap opening at the Dirac points for the monolayer [8, 9].

While graphene is highly conductive in-plane, its conductivity perpendicular to the plane is actually low [10]. The statement of graphene being conductive while h-BN being insulating is essentially relevant to the in-plane electronic structure (see supplementary section, figure S3). In order to study the electron transport through the plane, it is necessary to build an 'electrode-graphene/BN-electrode' configuration, analogous to a molecular junction, where graphene or BN functions as a 2D 'molecule' connected to two electrodes. In fact, several recent investigations have reported the perpendicular electron tunneling properties of BN and graphene, primarily because of research interest in graphene engineering [11–18].

For the case of multilayer boron nitride, Lee *et al* have used a Pt tip in the atomic force microscopy experiments to measure the current penetrating the h-BN layers, which were

deposited on a gold substrate [13]. Britnell *et al* have used a symmetric configuration in which the h-BN monolayer was sandwiched between two similar electrodes [11, 12]. Both studies reported approximately linear *I–V* characteristics at low bias, and thereafter a sharp increase of the tunneling current beyond the breakdown voltage. The observed tunneling features [13] were also confirmed by theoretical studies in which multilayer h-BN was sandwiched between graphene electrodes [14, 15, 19].

The 'electrode–graphene–electrode' configuration is recently fabricated to show that a low-resistance spin injection into n-doped silicon can be achieved by using graphene as the tunnel barrier [16, 17]. Theoretically, the vertical electron transport across multilayer graphene sandwiched between metal electrodes was studied [18]. It was shown that the conductance of graphene decays exponentially with increasing number of layers for some metals, similar to the results obtained for the h-BN monolayer sandwiched between graphene electrodes [12, 14, 15, 19].

In the light of the similar tunneling characteristics between the metal–graphene–metal configuration and the graphene–BN–graphene configuration, one can ask the question about the vertical electronic transport of graphene versus the layered h-BN employing the same configuration. Such a question is addressed in this work using the configurations consisted of graphene or h-BN with gold contacts. We consider the atomically flat gold contacts [20] with an aim to focus on the difference between graphene/gold interface and h-BN/gold interface. Since h-BN has a large band gap while graphene is gapless, one would initially infer that the tunneling current penetrating graphene is considerably larger than that penetrating h-BN. We will show that this is not the case. Both monolayers coupled with gold contacts exhibit similar transmittance characteristics, implying that the electron transport properties are dominated by the coupling of electrode-monolayer at the interface.

2. Computational methods

The prototypical configurations for our electron transport calculations are shown in figure 1. Six underlying substrate gold (111) layers and six probe gold (111) layers atop are taken to design the contact electrodes to avoid any unphysical charge leakage through the device configuration. The (111) surface is chosen because it is the energetically preferred surface for gold [21]. We have considered a (2×1) commensurate geometry for the graphene/gold and h-BN/gold interfaces, consisting of a (2×2) supercell of graphene or h-BN and a (1×1) supercell of the probe and substrate gold electrodes, respectively. The choice of the gold contacts is based on a recent result suggesting weakly interacting metals such as gold facilitates to keep the intrinsic π band structure of graphene [22]. Furthermore, the previously reported DFT calculations have considered similar graphene/BN-metal interfaces with satisfactory results [23–26]. Note that the DFT calculations are known to underestimate the band gap for semiconducting and ionic materials, though they provide

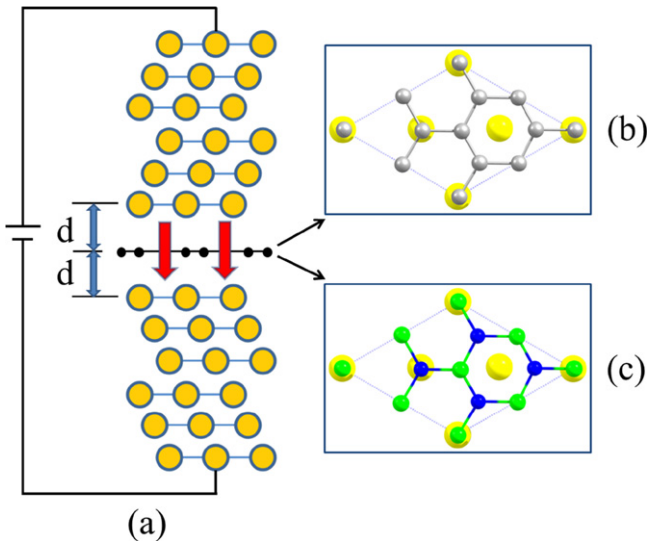

Figure 1. (a) The configuration used for the vertical electron transport properties in which either graphene or h-BN, is symmetrically sandwiched between two Au-(111) contacts. (b) The contact details of gold (111) surface with (b) graphene, and (c) h-BN monolayer. Yellow: gold; gray: carbon; blue: nitrogen; and green: boron.

accurate and reliable description of the nature of valance and conduction bands.

The electronic structure of the graphene or h-BN layers was obtained in the framework of the local density approximation (LDA) for the exchange and correlation functional as implemented in the SIESTA computational code [27, 28]. Norm-conserving pseudo-potential and double-zeta basis sets with polarization functions were used for all atoms in the calculations. All structures were fully relaxed until the residual forces in each atom component were smaller than 0.01 eV $Å^{-1}$. The calculated lattice constants are 2.46 and 2.49 Å for graphene and h-BN monolayer, respectively, consistent with our previous work [8]. It leads to a small mismatch of no greater than 1.6% between the Au (111) surface and graphene or h-BN layer. A grid of 100×100 *k*-points, perpendicular to the tunneling direction was used for the electronic transport calculations. The zero bias total transmission is subsequently calculated using the non-equilibrium Green's function (NEGF) method [29], as implemented in the Transiesta package [30, 31].

3. Results and discussions

We first seek to determine the equilibrium distance between the contact and the monolayer for the configuration where the monolayer is symmetrically positioned between the gold (111) surface contacts. The equilibrium spacing is calculated to be 3.1 Å (see supplementary section, figure S2), and the calculated binding energies of the configurations considered compare well with the results of previous studies [24, 26]. No buckling in the atomic layer is expected because of the spatial symmetry of the interface—the forces acting on the layer

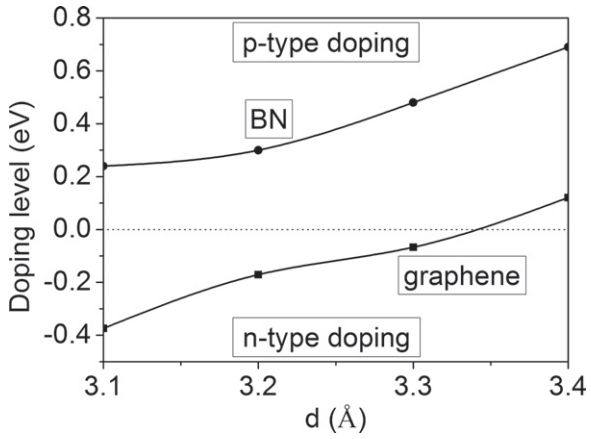

Figure 2. Doping level *versus* the contact-monolayer distance for the devices considered. The dotted line aligned at zero refers to the pristine case.

induced by the upper probe contact are balanced by those induced by the substrate contact. A stronger binding of Au with graphene relative to that of the h-BN monolayer is predicted which is also consistent with previous studies on adsorption of transition-metal atoms and biomolecules on the tubular configurations of C and BN [32, 33].

Graphene has a zero energy gap, and h-BN shows a finite gap. Only the 2p electrons of the constituent atoms contribute to the states forming the valance band maximum (VBM) and the conduction band minimum (CBM). When the interface of the monolayer with gold contacts begins to form with the interface distance being 4.0 Å, bonding is relatively weak, as evidenced by the nearly unchanged PDOS of graphene and h-BN monolayer (see supplementary section, figure S2). However, there exists a charge transfer for Au-graphene-Au that puts the charge neutrality point above the Fermi level, consequently suggesting the doping to be p-type in graphene. We find that the bonding between contact-monolayer becomes stronger as the interface distance becomes smaller which, in turn, modifies density of states.

Figure 2 shows the variation of the doping level with the contact-monolayer distance at the interface for the configurations considered. For graphene, the doping level is defined by a shift in the Dirac point with respect to the Fermi level, while the doping level of the h-BN monolayer is given by the shift of the midpoint between VBM and CBM with respect to the Fermi level. A weak coupling at the interface (i.e. distance =4.0 Å) induces p-type doping in the Au–graphene–Au device. This is due to dissimilar work functions between gold (111) surface and graphene, as also reported previously [25, 26, 34].

As we decrease the contact-monolayer distance to 3.1 Å, p-type doping becomes n-type doping in Au–graphene–Au (figure 4). It is worth noting that the Dirac point of graphene (at ~ -0.37 eV) can still be tracked as the local minimum in the vicinity of the Fermi level for the equilibrium interface distance, though finite DOS suggests a higher degree of hybridization of C states with Au states. This hybridization is also manifested by the less-smooth PDOS (figure S3 (3.1 Å) in the supplementary material) relative to that representing the graphene-gold coupling regime (figure S3 (4.0 Å) in the supplementary material). These results are consistent with the previously reported scanning tunneling spectroscopy studies [35].

The Au–BN–Au device shows the p-type doping at the equilibrium distance (figure 2), though there is a global shift of electronic states to the right in the weak coupling regime (4.0 Å) which can be quantified by tracking the midpoint of VBM and CBM. For the contact-monolayer distance of 3.4 and 3.1 Å, the doping level is calculated to be at 0.69 and 0.23 eV, respectively (figure 2). The p-type doping effect is further confirmed by Mulliken population analysis which finds transfer of electron from B to Au; electron transfer being 0.14 e B^{-1} atom at the equilibrium spacing of 3.1 Å. These results are consistent with the previously reported studies on the electron transport in boron nanostructures including boron nanotubes and boron fullerenes [36, 37]. A distinct nature of the electronic structure is therefore predicted for both devices, specifically at the equilibrium contact-monolayer distance at the interface.

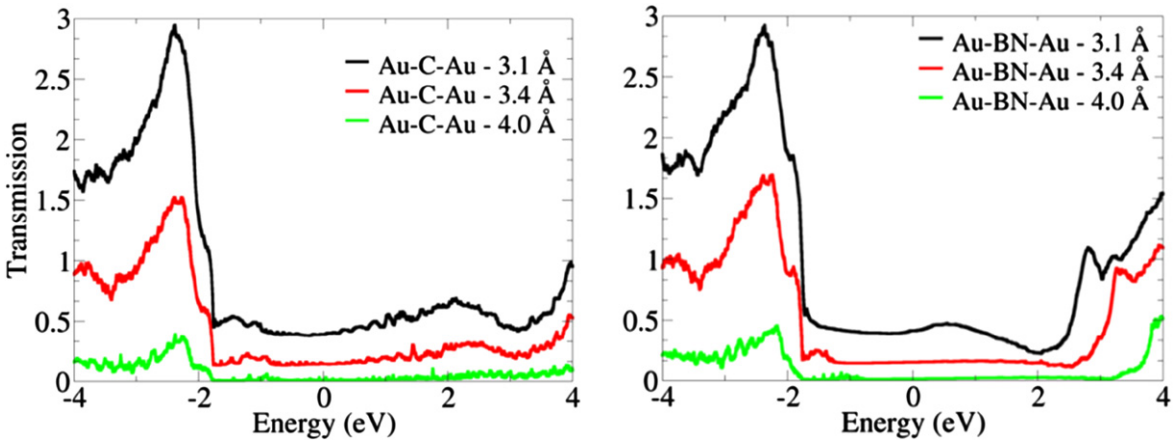

Figure 3. The characteristic transmission functions of the Au–graphene monolayer–Au and Au–BN monolayer–Au configurations. Fermi level of the device is aligned to zero.

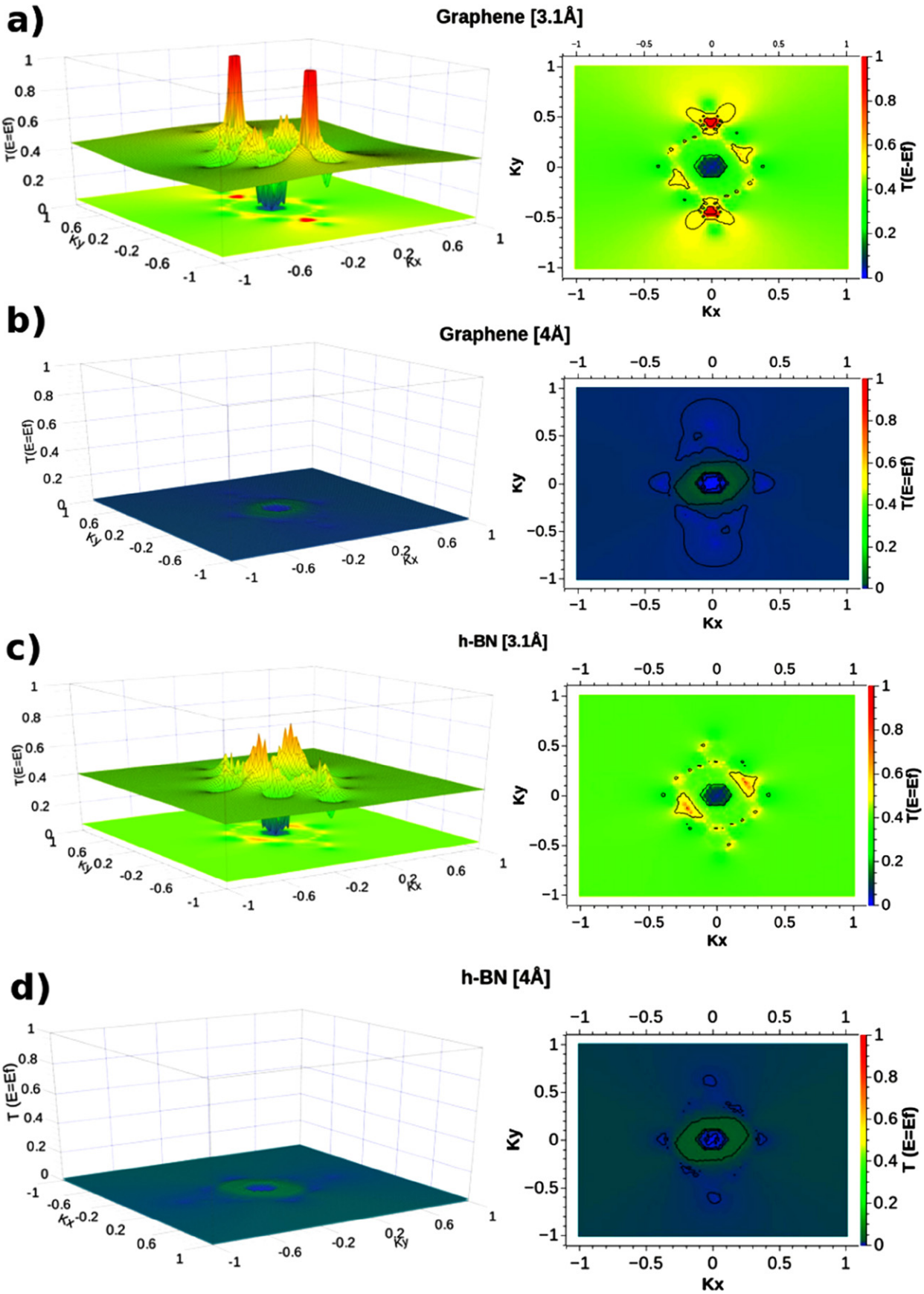

Figure 4. (Left panel) The *k*-point (k_x, k_y) *versus* transmission function at Fermi level for graphene and h-BN monolayer at the contact-monolayer distances of 3.1 and 4.0 Å. (Right panel) The projection of the left panel on the k_x, k_y axis. The accompanying color scale indicates values of the transmission function at Fermi level.

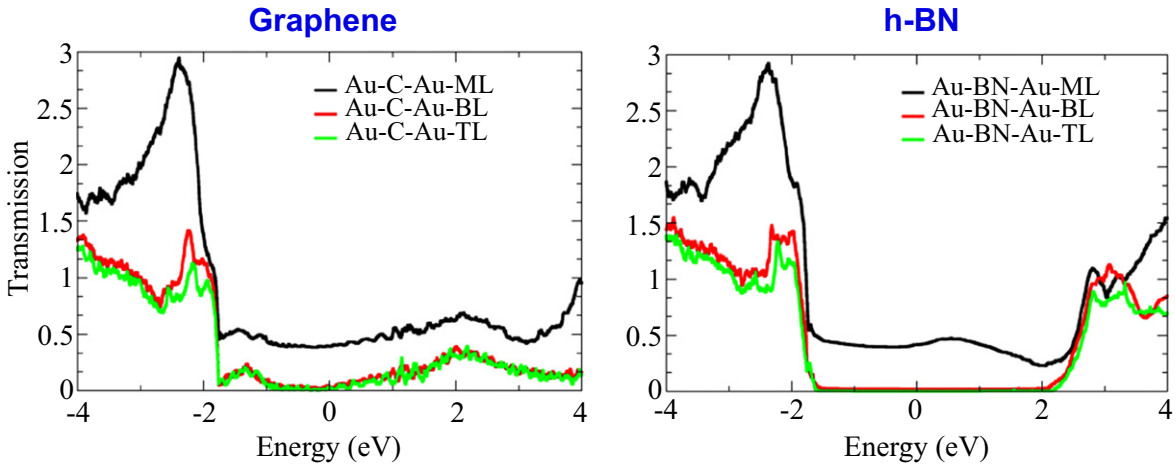

Figure 5. The evolution of characteristic transmission functions of the Au–graphene–Au and Au–BN–Au configurations with respect to the number of layers. ML-monolayer, BL-bilayer, and TL-trilayer.

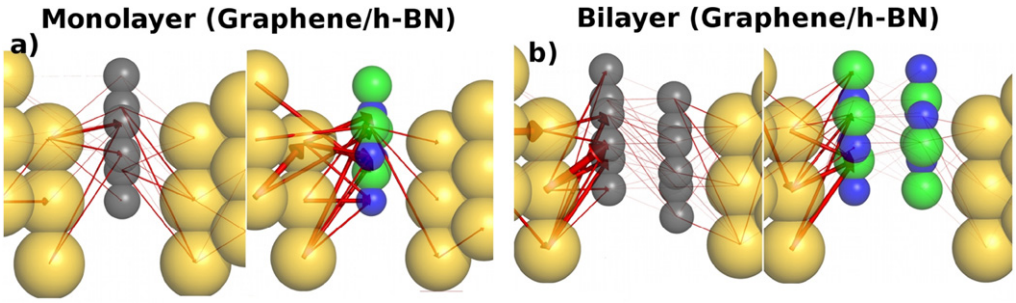

Figure 6. Local currents for (a) monolayer graphene (h-BN) and (b) bilayer graphene (h-BN).

The electronic transmission functions are shown in figure 3. At the contact-monolayer distance of 4.0 Å, dominance of electron tunneling is clearly seen with a number of resonance peaks for graphene. Such resonance peaks are not present for h-BN near the Fermi level. At the equilibrium distance of 3.1 Å, the magnitude of the transmission function is nearly the same at the Fermi level for both devices suggesting them to be equally conductive, though pristine graphene is semi-metal and h-BN monolayer is semiconducting [38]. The calculated results therefore attribute a higher order of the conductivity associated with Au–BN–Au to a relatively strong hybridization of the monolayer with Au contacts which, in turn, renders a finite density of states around the Fermi level of the system.

In order to corroborate the above-mentioned discussion, we now show the *k*-point resolved transmission coefficients at the Fermi level in figure 4. For both cases, the transmission coefficients are nearly the same except for *K* and *K′* points in the reciprocal space. Once integrated over the entire Brillouin zone in the reciprocal space, the effects of those resonances are washed away and a similar conductance is obtained for the configurations consisting of either a graphene or h-BN monolayer sandwiched between Au contacts.

We now replace the monolayer by multilayers to examine the dependence of the transmission function on the number of layers (figure 5). The results are also expected to reveal subtle effects introduced by the interfacial bonding in the configuration considered. Note that the *AA′* stacking is considered for multilayer BN whereas the AB (Bernal) stacking is taken for multilayer graphene [39]. The interlayer distance between adjacent layers is set as 3.3 Å for both graphene and h-BN multilayers [39, 40], while the interface distance between the outermost layer of graphene or BN and gold is set as 3.1 Å, the same as Au–graphene/BN monolayer–Au configurations.

Table 1. Zero-bias conductance of multilayers of graphene and h-BN given in units of G_0.

	Graphene	h-BN
Monolayer	0.392	0.414
Bilayer	0.032	0.018
Trilayer	0.027	0.001

The results find a significant drop in the transmission function for BN in going from monolayer to bilayer in line with the results of previous studies using graphene as electrodes [12, 14, 15, 19]. On the other hand, the transmission function of bilayer graphene is about an order of magnitude smaller than that of monolayer graphene in the low bias regime, as also reported previously [18]. Calculations of the zero-bias conductance find that the conductance of the h-BN monolayer to be about 6% larger than that of graphene. This is not the case with bilayers and trilayers, where the out-of-plane conductance is significantly larger for graphene.

Figure 6 shows the local currents flowing from the left electrode across either the monolayer or the bilayer indicating that the current density between layers is relatively low for the h-BN bilayer relative to that of the monolayer. The calculated zero-bias conductance of the multilayer considered given in table 1 reaffirms the scenario shown in figure 6. The exponential dependence of the conductance in h-BN is predicted. We also find that bilayer or trilayer of graphene is more conducting than those of BN. Therefore, a significant suppression of tunneling current for the h-BN bilayer or trilayer suggests that while graphene and the h-BN monolayer have similar interface binding strength with gold electrodes, the interlayer coupling between adjacent layers of graphene is much stronger than that of h-BN layers in terms of the out-of-plane electron transport.

4. Summary

Calculations using the LDA-DFT level of theory together with the NEGF method were performed on gold–graphene–gold and gold–BN–gold configurations to investigate their vertical electron transmission characteristics. The electron deficient nature of boron induces a strong coupling of h-BN monolayer with gold contacts which modifies the electronic properties of the pristine h-BN monolayer. We find a stronger tendency of *p*-doping of h-BN in the Au–BN–Au device which persists at the equilibrium contact-monolayer distance of 3.1 Å. This is in contrast to the case of Au–graphene–Au where *n*-type doping is predicted at the equilibrium contact-monolayer distance at the interface.

In spite of a distinctly different nature of the electronic properties of pristine graphene and h-BN monolayer, the conductance properties of both layers coupled with gold contacts are predicted to be very similar. A relative strong coupling between Au contacts and h-BN monolayer leads to a transmission channel at the Fermi level together with the fact that the influence of the Dirac point is small when integrated over the entire Brillouin zone for the out-of-plane conductance in the Au–graphene–Au device. As a consequence, one would not expect single layer h-BN coupled with atomically flat weakly interacting metals such as gold to work as a good dielectric material, but the absence of sharp resonances would probably lead to more stable transverse electronic transport properties compared to graphene. The h-BN multilayers exhibit an exponential decay of transmission function in going from monolayer to bilayer to trilayer, whereas multilayer graphene shows higher tunneling probability due to a stronger interlayer coupling between adjacent layers. The present study, therefore, delineates the in-plane and out-of-the-plane electron transport properties of graphene and h-BN coupled with gold contacts for applications in nanoscale devices.

Acknowledgment

We acknowledge support from Brazilian Agencies CNPq and FAPESP (grant # 2009/07095-1) and computational resources CENAPAD/SP and NACAD/UFRJ.

References

[1] Rogers J A, Lagally M G and Nuzzo R G 2011 Synthesis, assembly and applications of semiconductor nanomembranes *Nature* **477** 45–53
[2] Geim A K and Novoselov K S 2007 The rise of graphene *Nat. Mater.* **6** 183–91
[3] Novoselov K S *et al* 2005 Two-dimensional atomic crystals *Proc. Natl Acad. Sci. USA* **102** 10451–3
[4] Bourzac K 2012 Electronics: back to analogue *Nature* **483** S34–6
[5] Bolotin K I *et al* 2008 Ultrahigh electron mobility in suspended graphene *Solid State Commun.* **146** 351–5
[6] Song L *et al* 2010 Large scale growth and characterization of atomic hexagonal boron nitride layers *Nano Lett.* **10** 3209–15
[7] Castro Neto A H *et al* 2009 The electronic properties of graphene *Rev. Mod. Phys.* **81** 109
[8] Şahin H *et al* 2009 Monolayer honeycomb structures of group-IV elements and III-V binary compounds: first-principles calculations *Phys. Rev.* B **80** 155453
[9] Zhong X *et al* 2011 First-principles study of strain-induced modulation of energy gaps of graphene/BN and BN bilayers *Phys. Rev.* B **83** 193403
[10] Krishnan K and Ganguli N 1939 Large anisotropy of the electrical conductivity of graphite *Nature* **144** 667
[11] Britnell L *et al* 2012 Field-effect tunneling transistor based on vertical graphene heterostructures *Science* **335** 947–50
[12] Britnell L *et al* 2012 Electron tunneling through ultrathin boron nitride crystalline barriers *Nano Lett.* **12** 1707–10
[13] Lee G-H *et al* 2011 Electron tunneling through atomically flat and ultrathin hexagonal boron nitride *Appl. Phys. Lett.* **99** 243114–3
[14] Vasko F T 2013 Resonant and nondissipative tunneling in independently contacted graphene structures *Phys. Rev.* B **87** 075424
[15] Kumar S B, Seol G and Guo J 2012 Modeling of a vertical tunneling graphene heterojunction field-effect transistor *Appl. Phys. Lett.* **101** 033503–5
[16] van't Erve O M J *et al* 2012 Low-resistance spin injection into silicon using graphene tunnel barriers *Nat. Nanotechnology* **7** 737–42
[17] Dery H 2012 Spin injection graphene wins the match *Nat. Nanotechnology.* **7** 692–3
[18] Kuroda M A *et al* 2011 Conductance through multilayer graphene films *Nano Lett.* **11** 3629–33
[19] Bruzzone S, Fiori G and Iannaccone G 2012 Tunneling properties of vertical heterostructures of multilayer hexagonal boron nitride and graphene arXiv: 1212.4629
[20] Huang J-S *et al* 2010 Atomically flat single-crystalline gold nanostructures for plasmonic nanocircuitry *Nat. Commun.* **1** 150
[21] Rodrigues V, Fuhrer T and Ugarte D 2000 Signature of atomic structure in the quantum conductance of gold nanowires *Phys. Rev. Lett.* **85** 4124–7
[22] Gong C *et al* 2012 Metal–graphene–metal sandwich contacts for enhanced interface bonding and work function control *ACS Nano.* **6** 5381–7
[23] Grad G B *et al* 2003 Density functional theory investigation of the geometric and spintronic structure of h-BN/Ni(111) in view of photoemission and STM experiments *Phys. Rev.* B **68** 085404
[24] Laskowski R, Blaha P and Schwarz K 2008 Bonding of hexagonal BN to transition metal surfaces: an *ab initio* density-functional theory study *Phys. Rev.* B **78** 045409
[25] Khomyakov P A *et al* 2009 First-principles study of the interaction and charge transfer between graphene and metals *Phys. Rev.* B **79** 195425
[26] Sławińska J, Dabrowski P and Zasada I 2011 Doping of graphene by a Au(111) substrate: calculation strategy within

the local density approximation and a semiempirical van der Waals approach *Phys. Rev.* B **83** 245429
[27] SanchezPortal D *et al* 1997 Density-functional method for very large systems with LCAO basis sets *Int. J. Quant. Chem.* **65** 453–61
[28] José M S *et al* 2002 The SIESTA method for ab initio order- N materials simulation *J. Phys.: Condens. Matter* **14** 2745
[29] Datta S 1997 *Electronic Transport in Mesoscopic Systems* (Cambridge: Cambridge University Press)
[30] Brandbyge M *et al* 2002 Density-functional method for nonequilibrium electron transport *Phys. Rev.* B **65** 165401
[31] Nakamura H *et al* 2008 Efficient *ab initio* method for inelastic transport in nanoscale devices: analysis of inelastic electron tunneling spectroscopy *Phys. Rev.* B **78** 235420
[32] Wu X and Zeng X C 2006 Adsorption of transition-metal atoms on boron nitride nanotube: a density-functional study *J. Chem. Phys.* **125** 044711–7
[33] Durgun E *et al* 2003 Systematic study of adsorption of single atoms on a carbon nanotube *Phys. Rev.* B **67** 201401
[34] Giovannetti G *et al* 2008 Doping graphene with metal contacts *Phys. Rev. Lett.* **101** 026803
[35] Klusek Z *et al* 2009 Graphene on gold: electron density of states studies by scanning tunneling spectroscopy *Appl. Phys. Lett.* **95** 113114–3
[36] Lau K C *et al* 2006 Theoretical study of electron transport in boron nanotubes *Appl. Phys. Lett* **88** 212111–3
[37] He H *et al* 2010 Metal-like electrical conductance in boron fullerenes *J. Phys. Chem.* C **114** 4149–52
[38] Amorim R G *et al* 2013 Strain- and electric field-induced band gap modulation in nitride nanomembranes *J. Phys.: Condens. Matter* **25** 195801
[39] Hod O 2012 Graphite and hexagonal boron-nitride have the same interlayer distance. why? *J. Chem. Theory Comput.* **8** 1360–9
[40] Zhong X *et al* 2012 Electronic structure and quantum transport properties of trilayers formed from graphene and boron nitride *Nanoscale* **4** 5490–8

Supplementary Section:

The out-of-plane electron tunneling properties of graphene and h-BN monolayers

Xiaoliang Zhong[1], Rodrigo G. Amorim[2], Alexandre R. Rocha[3*], Ravindra Pandey[1]*

[1]*Department of Physics, Michigan Technological University, Houghton, Michigan, 49931, U.S.A*

[2]*Physics Department, Uppsala University, Uppsala, Sweden*

[3]*Instituto de Física Teórica, Universidade Estadual Paulista (UNESP), Sao Paulo, SP, Brazil*

Figure S1 shows a variation of the binding energy (E_B) of the system with the contact-monolayer distance at the interface. E_B is defined as the total energy of a gold-monolayer-gold system subtracted by the sum of total energies of the corresponding gold capacitor and the isolated layer.

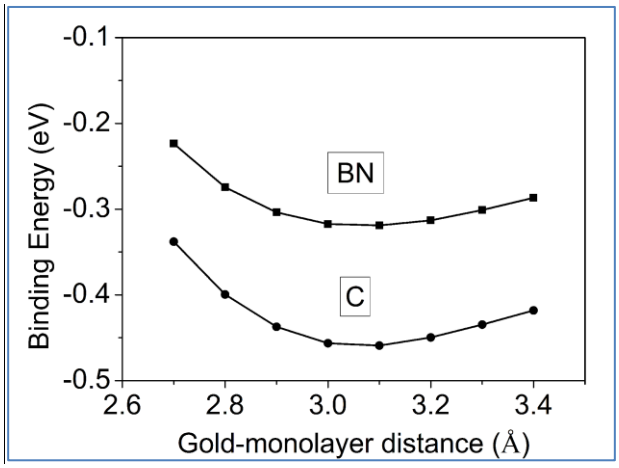

Figure S1. *Binding energy (E_B) per formula unit vs. the interface distance for the configuration.*

The atomically projected density of states (PDOS) is shown in Figure S2. Graphene has a zero energy gap, and h-BN shows a finite gap. Only the 2p electrons of the constituent atoms contribute to the states forming the valance band maximum (VBM) and the conduction band minimum (CBM). When the interface of the monolayer with gold contacts begins to form with the interface distance being 4.0 Å, bonding is relatively weak, as evidenced by the nearly unchanged PDOS of graphene and h-BN monolayer. However, there exists a charge transfer for Au-graphene-Au that puts the charge neutrality point above the Fermi level, consequently suggesting the doping to be p-type in graphene. We find that the bonding between contact-monolayer becomes stronger as the interface distance becomes smaller which, in turn, modifies density of states (Figure S2).

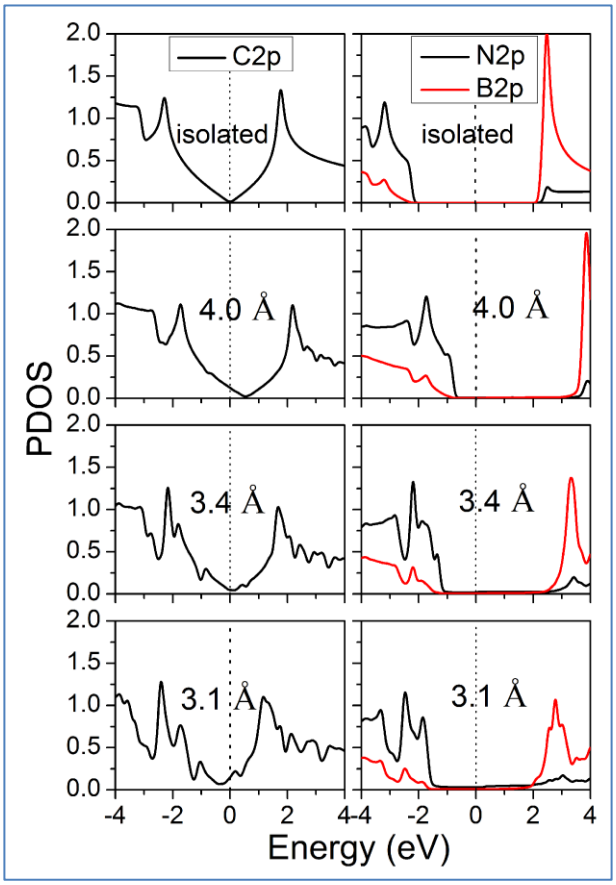

Figure S2. *The projected density of states vs. the contact-monolayer distance at the interface: Au-graphene–Au (left), Au-BN-Au (right). Zero of energy is aligned to the Fermi level of the system.*

The in-plane transmittance of isolated graphene and h-BN monolayers are given in Fig. S3, showing their distinct electronic properties. It is clear from Fig. S3 that while graphene is a zero gap semiconductor, h-BN has a wide gap of approximately 4 eV. This gap is also observed in the density of states given in Fig S2 for the pristine h-BN monolayer.

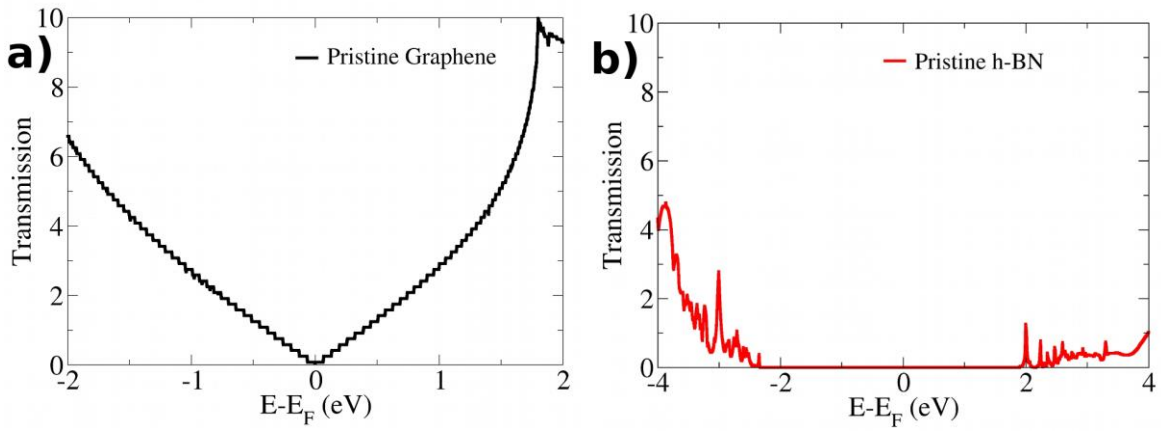

Figure S3. *The in-plane transmittance of graphene and BN monolayers.*